Journal of Photochemistry and Photobiology A: Chemistry 214 (2010) 92–99

Contents lists available at ScienceDirect

Journal of Photochemistry and Photobiology A: Chemistry

journal homepage: www.elsevier.com/locate/jphotochem

Synthesis, crystal structures and fluorescence properties of 3-(2-pyridyl)coumarin derivatives

Tianzhi Yu[a,*], Sidan Yang[a,b], Yuling Zhao[b], Hui Zhang[a], Xiaoqian Han[b], Duowang Fan[a], Yongqing Qiu[c], Lili Chen[c]

[a] Key Laboratory of Opto-Electronic Technology and Intelligent Control (Lanzhou Jiaotong University), Ministry of Education, Lanzhou 730070, China
[b] School of Chemical and Biological Engineering, Lanzhou Jiaotong University, Lanzhou 730070, China
[c] Institute of Functional Material Chemistry, Faculty of Chemistry, Northeast Normal University, Changchun 130024, China

ARTICLE INFO

Article history:
Received 15 December 2009
Received in revised form 3 June 2010
Accepted 16 June 2010
Available online 23 June 2010

Keywords:
Synthesis
Crystal structure
3-(2-Pyridyl)coumarin derivatives
Fluorescence

ABSTRACT

Two new coumarin derivatives, 7-(diethylamino)-3-(pyridin-2-yl)coumarin (DAPC) and 3-(pyridin-2-yl)-benzo[5,6]coumarin (PBC), were synthesized and characterized by elemental analysis, ^{1}H NMR, FT-IR and UV–vis absorption spectra. Their structures were determined by X-ray crystallography single crystal analysis. The fluorescence behaviors of the compounds in dichloromethane solutions were observed. The results show that the compound DAPC exhibits high fluorescence quantum yield (0.84) and they exhibit strong blue emissions under ultraviolet light excitation. The energy levels of the HOMO and LUMO of the compounds have been calculated with density functional theory (DFT) and time-dependent density functional theory (TD-DFT) at B3LYP/6-31G(d) level.

1. Introduction

It has been almost 200 years since coumarin was first reported and isolated from a number of plants [1]. To date, naturally occurring coumarins have been isolated from over 800 species of plants and microorganisms, and more than 1000 coumarin derivatives have been described [2]. Coumarin and its derivatives are an important class of organic compounds which not only play a significant role in pharmacological activity such as antibacterial, anti-HIV and anticancer activity [3–6], but also use in laser dyes, nonlinear optical chromophores, fluorescent whiteners, fluorescent probes and solar energy collectors due to their outstanding optical properties [7–11]. Coumarins owe their importance as fluorescent brightening agents and dyes to their efficient light emission properties, their reasonable stability and their relative ease of synthesis.

Strong fluorescence of coumarins is attributed to the charge transfer from the styryl to the carbonyloxy group [12]. Their absorption and fluorescence characteristics are strongly altered by the nature of substituents, substituted position in the coumarin ring and solvents [13]. Electron attracting groups in the 3-position and electron repelling groups in the 7-position have been shown to enhance the fluorescence intensity of coumarins [14].

Although several coumarin derivatives which possess good photoluminescence ($\Phi_F > 0.5$) and electroluminescence properties were investigated in our laboratory [15–19], there remain some interests in the molecular design and synthesis of new coumarin derivatives with high quantum yield of fluorescence and greater stability. The present work is a continuation of our search on high efficient emitting fluorescent materials. Thus we have synthesized two new coumarin derivatives, 7-(diethylamino)-3-(pyridin-2-yl)coumarin (DAPC) and 3-(pyridin-2-yl)-benzo[5,6]coumarin (PBC). The strategy is to attach an electron-attracting moiety (2-pyridyl) in the 3-position of the coumarin which is expected to enhance the fluorescence efficiency of coumarins [17]. Another reason is to obtain new ligands for Ir (III) complexes which is being undertaken in our laboratory, because the Ir (III) coumarin complexes possess higher quantum yields and much higher brightnesses [20,21]. In this communication, we report the photophysical properties of DAPC and PBC in diluted dichloromethane solutions. The compounds exhibit strong blue emissions under ultraviolet light excitation.

2. Experimental

2.1. Materials and methods

4-(N,N′-Diethylamino)salicylaldehyde was bought from Zhejiang Huadee Dyestuff Chemical Co. Ltd. (China) and was recrystallized from ethanol. 2-Hydroxy-1-naphthaldehyde and

* Corresponding author. Tel.: +86 931 4956935; fax: +86 931 4938756.
E-mail address: ytz823@hotmail.com (T. Yu).

1010-6030/$ – see front matter © 2010 Elsevier B.V. All rights reserved.
doi:10.1016/j.jphotochem.2010.06.013

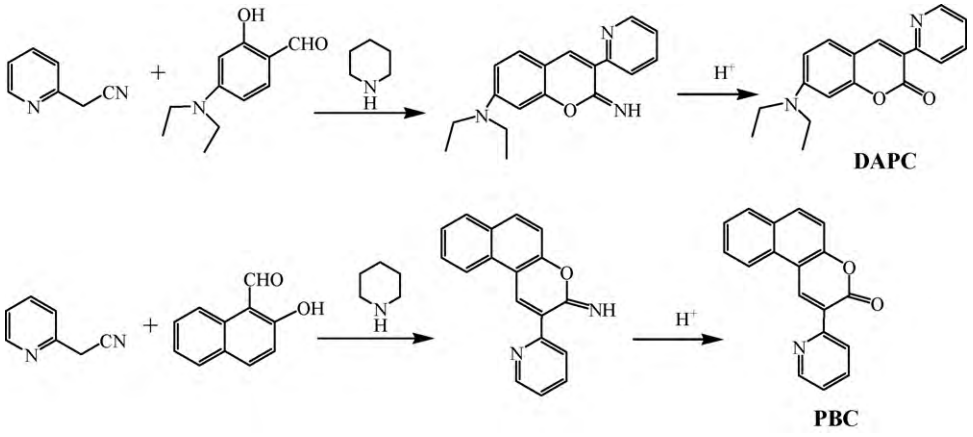

Scheme 1. Synthetic routines to the compounds DAPC and PBC.

pyridine-2-acetonitrile were purchased from Alfa Aesar. All other chemicals were analytical grade reagent.

IR spectra (400–4000 cm^{-1}) were measured on a Shimadzu IRPrestige-21 FT-IR spectrophotometer. ^1H NMR spectra were obtained on Unity Varian-500 MHz. C, H, and N analyses were obtained using an Elemental Vario-EL automatic elemental analysis instrument. Mass spectra were recorded on a Gas Chromatography–Mass Spectrometry (Thermo Trace DSQ), using electron ionization at 70 eV. UV–vis absorption and emission spectra were recorded on a Shimadzu UV-2550 spectrometer and on a Perkin-Elmer LS-55 spectrometer, respectively. Fluorescence quantum yield of DAPC and PBC in acetonitrile were measured with anthracene as reference ($\Phi_F^S = 0.25$ [22]). The quantum yields (Φ_F) were calculated according to the literatures [22,23]. Melting points were measured by using an X-4 microscopic melting point apparatus made in Beijing Taike Instrument Limited Company, and the thermometer was uncorrected.

2.2. Synthesis and characterization of 7-(diethylamino)-3-(pyridin-2-yl)coumarin (DAPC) and 3-(pyridin-2-yl)-benzo[5,6]coumarin (PBC)

The synthetic routes were shown in Scheme 1. DAPC and PBC were synthesized according to the procedure described in literature [17].

7-(Diethylamino)-3-(pyridin-2-yl)coumarin. 4-(N,N′-Diethylamino)salicylaldehyde (1.93 g, 0.01 mol) and pyridine-2-acetonitrile (1.18 g, 0.01 mol) were dissolved in 20 mL of anhydrous alcohol, and then piperidine (0.6 mL) was added stepwise under ice bath. The mixture was stirred for 12 h under ice bath, then treated with HCl (50 mL, 3.5%) and refluxed for 8 h to hydrolyze the iminocoumarin. When the reaction was finished, the acidic solution was neutralized with aqueous ammonia until the pH was 7. The resulting solution was evaporated under reduced pressure to exclude ethanol and the residue was extracted by dichloromethane (50 mL × 3). The organic phase was washed with water (2 × 50 mL) and dried over anhydrous $MgSO_4$. After filtering, the filtrate was evaporated to dryness under reduced pressure. The crude was purified by chromatography on silica gel using ethyl acetate/petroleum ether (1:8, v/v) as the eluent to give DAPC (2.15 g, 73.1%). m.p. 113–114 °C. IR (KBr pellet cm^{-1}): 3042 (aryl-CH), 2980, 2928 (alkyl-CH), 1719 (C=O, lactone), 1617 (C=C), 1591, 1579, 1515, 1471, 1412, 1348, 1272 cm^{-1}; ^1H NMR ($CDCl_3$, δ, ppm): 8.73 (s, 1H, Aryl-H), 8.64 (d, 1H, J = 5.4, Aryl-H), 8.45 (d, 1H, J = 8.2, Aryl-H), 7.77–7.74 (m, 1H, Aryl-H), 7.43 (d, 1H, J = 8.4, Aryl-H), 7.28–7.24 (m, 1H, Aryl-H), 6.62 (d, 1H, J = 8.4, Aryl-H), 6.53 (s, 1H, Aryl-H), 3.45 (q, 4H, J = 7.6, $-CH_2-$), 1.24 (t, 6H, J = 7.6, $-CH_3$). MS-EI: m/z (%) 295 (11), 294 (57) [M^+], 280 (17), 279 (100), 251 (23), 222 (13), 207 (16), 202 (14), 167 (11), 149 (32), 133 (11), 132 (19), 131 (21), 125 (11), 116 (10), 114 (18), 111 (15), 109 (10), 103 (12), 97 (19), 95 (13), 91 (11), 85 (16), 83 (22), 81 (13), 77 (12), 71 (22), 70 (12), 69 (21), 57 (28), 55 (19), 44 (14), 43 (26), 41 (13), 40 (45). Anal. Calc. for $C_{18}H_{18}O_2N_2$ (%): C, 73.45; H, 6.16; N, 9.52. Found: C, 73.53; H, 6.12; N, 9.49.

3-(Pyridin-2-yl)-benzo[5,6]coumarin. The preparation of PBC was similar to that described for *DAPC*, which was obtained from 2-hydroxy-1-naphthaldehyde and pyridine-2-acetonitrile. The crude was purified by chromatography on silica gel using ethyl acetate/petroleum (1:6, v/v). Yield: 81.5%. m.p. 193–195 °C. IR (KBr pellet cm^{-1}): 3073 (Aryl-CH), 1726 (C=O, lactone), 1628 (C=C), 1570, 1557, 1467, 1428, 1350, 1285, 1214, 1110, 1085 cm^{-1}. ^1H NMR: ($CDCl_3$, δ, ppm): 9.71 (s, 1H, H-4), 8.77 (d, 1H, J = 5.3, Aryl-H), 8.549–8.545 (m, 2H, Aryl-H), 8.05 (d, 1H, J = 9.6, Aryl-H), 7.94 (d, 1H, J = 8, Aryl-H), 7.88–7.84 (m, 1H, Aryl-H), 7.79–7.72 (m, 1H, Aryl-H), 7.62 (d, 1H, J = 8, Aryl-H), 7.54 (d, 1H, J = 9.6, Aryl-H), 7.38–7.32 (m, 1H, Aryl-H). MS-EI: m/z (%) 274 (16), 273 (88) [M^+], 251 (19), 246 (19), 245 (100), 244 (12), 222 (11), 217 (21), 216 (29), 215 (11), 189 (16), 108 (30), 40 (20). Anal. Calc. for $C_{18}H_{11}O_2N$ (%): C, 79.11; H, 4.06; N, 5.13. Found: C, 79.16; H, 4.02; N, 5.18.

2.3. Crystallography

Suitable crystals of DAPC and PBC were obtained by evaporation of ethyl acetate solutions. The diffraction data were collected with a Bruker Smart Apex CCD area detector using a graphite monochromated Mo Kα radiation (λ = 0.71073 Å) at 20 °C. The structures of DAPC and PBC were solved by using the program SHELXL and Fourier difference techniques, and refined by full-matrix least-squares method on F^2. All hydrogen atoms were added theoretically. The crystals and experimental data of DAPC and PBC are shown in Table 1. The selected bond lengths and bond angles of DAPC and PBC are listed in Table 2.

2.4. Quantum chemical calculations

The structure of DAPC and PBC were optimized by semiempirical density functional theory (DFT) using a B3LYP/6-31G (d) basis set. The structural energies of DAPC and PBC were calculated at B3LYP/6-31G(d) levels. The structure optimization and energy calculations were performed with the GAUSSIAN 98 program.

Table 1
Crystallographic data for 7-(diethylamino)-3-(pyridin-2-yl)coumarin (DAPC) and 3-(pyridin-2-yl)-benzo[5,6]coumarin (PBC).

Compound	DAPC	PBC
Empirical formula	$C_{18}H_{18}N_2O_2$	$C_{18}H_{11}NO_2$
Formula weight	294.34	273.28
Temperature (K)	293(2)	293(2)
Wavelength (Å)	0.71073	0.71073
Crystal system	Triclinic	Monoclinic
Space group	*P*-1	$P2_1/c$
Unit cell dimensions		
a (Å)	9.3049(9)	14.2953(13)
b (Å)	12.8504(13)	6.1945(6)
c (Å)	14.5480(15)	16.1165(15)
α (°)	103.298(2)	90
β (°)	108.598(2)	112.9835(12)
γ (°)	98.013(2)	90
Volume (Å^3), *Z*	1561.2(3), 4	1313.9(2), 4
Density (calculated) (g/cm^3)	1.252,	1.382
Absorption coefficient (mm^{-1})	0.083	0.091
F (0 0 0)	624	568
Crystal size (mm)	0.33 × 0.21 × 0.09	0.27 × 0.18 × 0.11
θ range for data collected (°)	1.54–26.05	1.55–26.04
Limiting indices	$-11 \le h \le 11$, $-8 \le k \le 15$, $-17 \le l \le 17$	$-17 \le h \le 17$, $-6 \le k \le 7$, $-19 \le l \le 16$
Reflections collected	8830	7006
Independent reflections	6024 (R_{int} = 0.0181)	2590 (R_{int} = 0.0204)
Absorption correction	Semi-empirical from equivalents	Semi-empirical from equivalents
Max. and min. transmission	0.9926 and 0.9733	0.9901 and 0.9759
Refinement method	Full-matrix least-squares on F^2	Full-matrix least-squares on F^2
Data/restraints/parameters	6024/0/401	2590/0/190
Goodness-of-fit on F^2	1.021	1.017
Final *R* indices [$I > 2\sigma(I)$]	R_1 = 0.0480, wR_2 = 0.1216	R_1 = 0.0434, wR_2 = 0.1101
R indices (all data)	R_1 = 0.0709, wR_2 = 0.1386	R_1 = 0.0605, wR_2 = 0.1222
Largest diff. Peak and hole (e Å^{-3})	0.161 and −0.205	0.137 and −0.189

3. Results and discussion

3.1. X-ray crystal structures of DAPC and PBC

The crystal structures and packing diagrams of DAPC and PBC are given in Fig. 1, Fig. 2, Fig. 3 and Fig. 4, respectively. The crystal data and experimental details are shown in Table 1. The selected bond lengths and bond angles of DAPC and PBC are listed in Table 2.

Acceptable crystals of DAPC for X-ray analysis were obtained by slow evaporation of ethyl acetate solution, and the crystal structure was measured by X-ray crystallography. The crystal of DAPC belongs to the triclinic space group *P*-1, $a = 9.3049(9)$ Å, $b = 12.8504(13)$ Å, $c = 14.5480(15)$ Å, $\alpha = 103.298(2)°$, $\beta = 108.598(2)°$, $\gamma = 98.013(2)°$, $U = 1561.2(3)$ Å^3, $Z = 4$, $D_c = 1.252$ g cm^{-3}, $\mu = 0.083$ mm^{-1}. As shown in Fig. 1, it is remarkable that there are two asymmetric molecules in crystal structure of DAPC due to the different space configuration of two ethylic groups of diethylamine in 7-position of coumarin ring, and these two molecules are space conformers. Although the pyridine rings are not coplanar with the coumarin rings in these two molecules, the dihedral angles are very small (7.51° and 13.05°, respectively). In addition, the coumarin skeleton of one DAPC molecule vertically located with the coumarin ring of other DAPC molecule, and the dihedral angle is 85.59°. From the packing diagram of DAPC (Fig. 2), we can see that there are strong intermolecular π–π interactions between two anti-paralleled molecules in a unit crystal cell, the interplanar distance is about 3.34 Å. However the intermolecular interactions are disconnected between different unit cells in the crystal lattices and thus no intermolecular π–π stacking exist in the DAPC crystal.

Acceptable crystals of PBC for X-ray analysis were also obtained by slow evaporation of ethyl acetate solution. Compared with DAPC, the crystal of PBC belongs to the monoclinic space group $P2_1/c$, $a = 14.2953(13)$ Å, $b = 6.1945(6)$ Å, $c = 16.1165(15)$ Å, $\beta = 112.9835(12)$, $U = 1313.9(2)$ Å^3, $Z = 4$, $D_c = 1.382$ g cm^{-3}, $\mu = 0.091$ mm^{-1}. Dissimilarly, there is one molecule in crystal

Table 2
Experimental and calculated structural parameters of DAPC and PBC.

DAPC			PBC		
	Exp.	Calcd.		Exp.	Calcd.
Bond length (Å)			Bond length (Å)		
C5–C6	1.4824	1.4876	C5–C6	1.4888	1.4893
O2–C14	1.2058	1.2129	O2–C10	1.2058	1.2118
N1–C11	1.3694	1.3810			
N1–C15	1.4599	1.4642			
N1–C17	1.4581	1.4639			
Bond angles (°)			Bond angles (°)		
C5–C6–C7	120.404	119.799	C5–C6–C7	121.081	119.694
O1–C14–O2	114.106	115.306	O1–C10–O2	115.420	115.797
C15–N1–C11	121.243	120.881			
Dihedral angle (°)			Dihedral angle (°)		
N2–C5–C6–C7	7.513	0.740	N1–C5–C6–C7	14.835	0.012

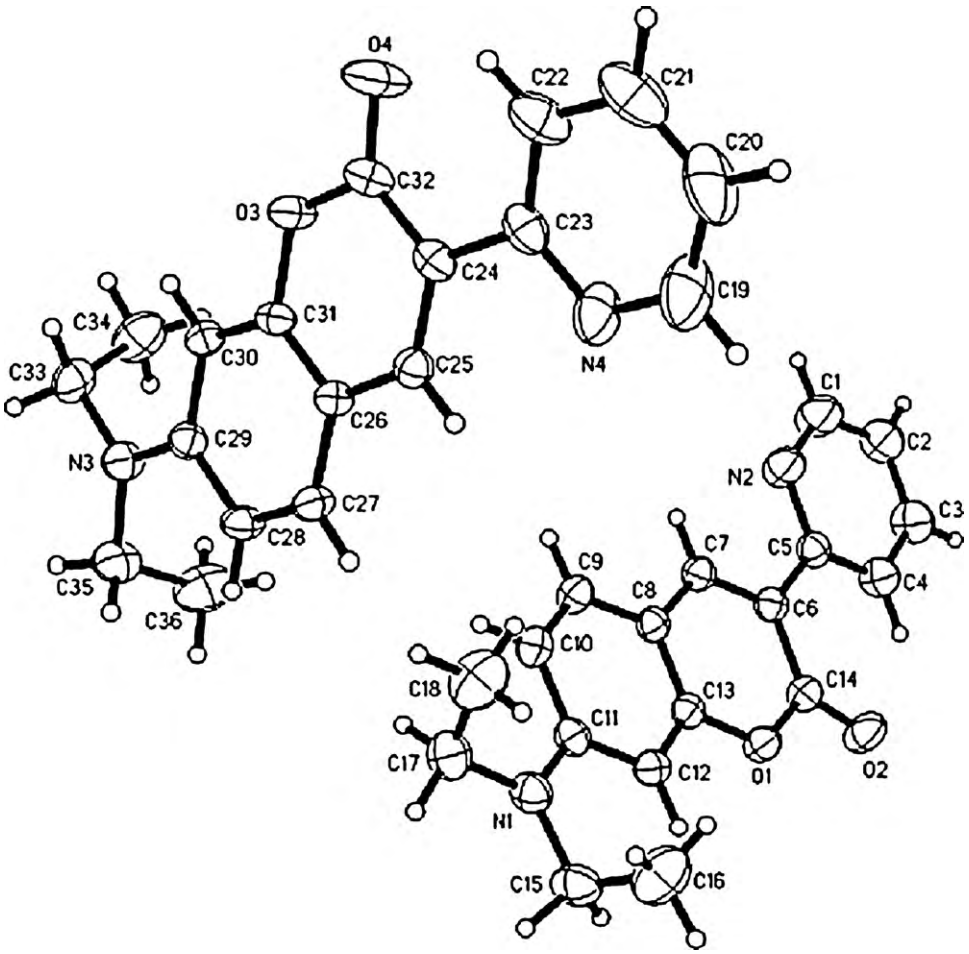

Fig. 1. Crystal structure of DAPC.

structure of PBC (Fig. 3). In the molecule, the pyridine ring is also not coplanar with the benzocoumarin skeleton and the dihedral angle is 14.84°. From Fig. 4, there is no intermolecular π–π stacking interaction between PBC molecules in crystal lattices.

3.2. UV–vis absorption and fluorescence of DAPC and PBC

UV–vis absorption spectra of the compound DAPC and PBC in diluted dichloromethane solutions are given in Fig. 5. It is shown

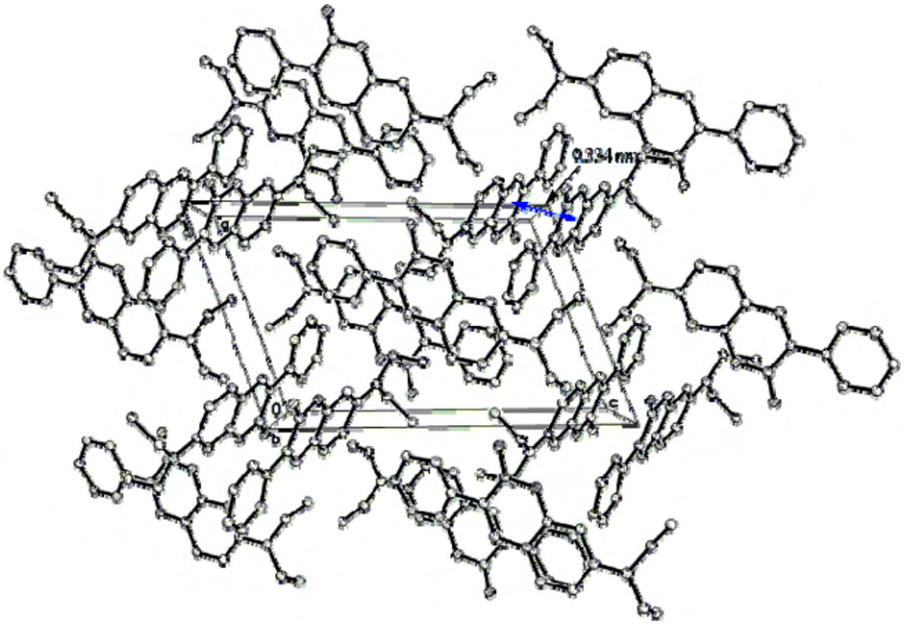

Fig. 2. Packing diagram of DAPC. H atoms are omitted for clarity.

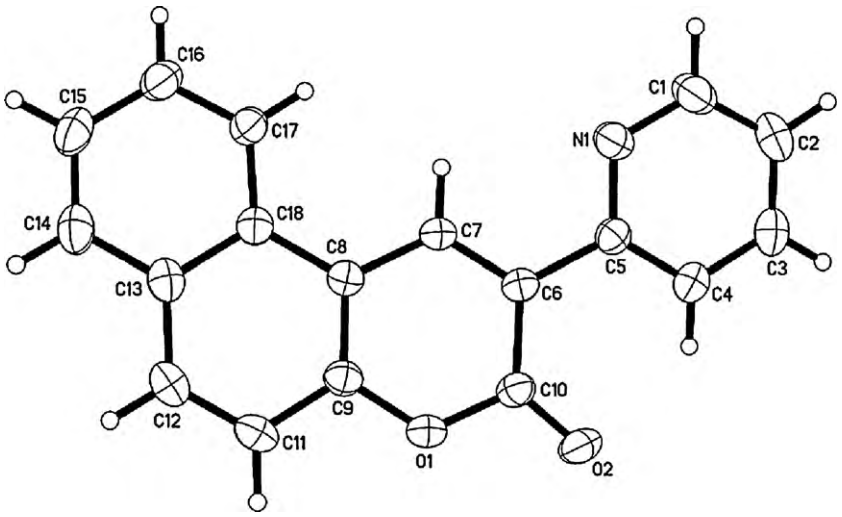

Fig. 3. Crystal structure of PBC.

that the absorption spectrum of DAPC exhibits absorption maxima at 236, 273 and 414 nm, respectively. The absorption spectrum of PBC shows absorption maxima at 242, 264 and 377 nm, respectively. Compared with DAPC, the absorption bands of PBC were blue-shifted. It is suggesting that the compound DAPC has an electron repelling diethylamine in the 7-position which enhances the electron density of coumarin ring, however, the compound PBC has a benzocoumarin skeleton which disperses the electron density of coumarin ring, so the absorption bands of PBC were blue-shifted compared to that of DAPC.

Fig. 5 also shows the emission spectra of DAPC and PBC in diluted dichloromethane solutions. It is shown that the compound DAPC exhibits bright blue emission with peak at 462 nm and the compound PBC shows bright blue emission at 441 nm and two additional shoulder peaks at 419 and 470 nm in dilute solution. The maximum emission wavelength of DAPC was bathochromically shifted by about 21 nm compared with that of PBC due to an electron repelling diethylamine in the 7-position in DAPC molecule. From the excitation and emission maxima of DAPC and PBC, the Stoke's shifts of DAPC and PBC are 2510 and 3850 cm^{-1}, respectively. The compound PBC has a larger Stoke's shift.

The emission behaviors of DAPC and PBC versus the concentrations in dichloromethane solutions were shown in Fig. 6. The emission peaks of DAPC and PBC are located at around 462 and 440 nm, respectively. It was found that the emission spectral features of DAPC and PBC changed with the solution concentrations. The concentration required for the maximum emission intensity was different in DAPC and PBC, which implies that concentration plays an important role in the different dye molecules. It is noticed that there is the strongest blue emission at about concentration of 8.0×10^{-6} mol/L for DAPC and 5.0×10^{-5} mol/L for PBC, respectively. When the concentrations were lower than these concentrations, the relative emission intensities increased gradually with increasing the concentrations. When the concentrations were

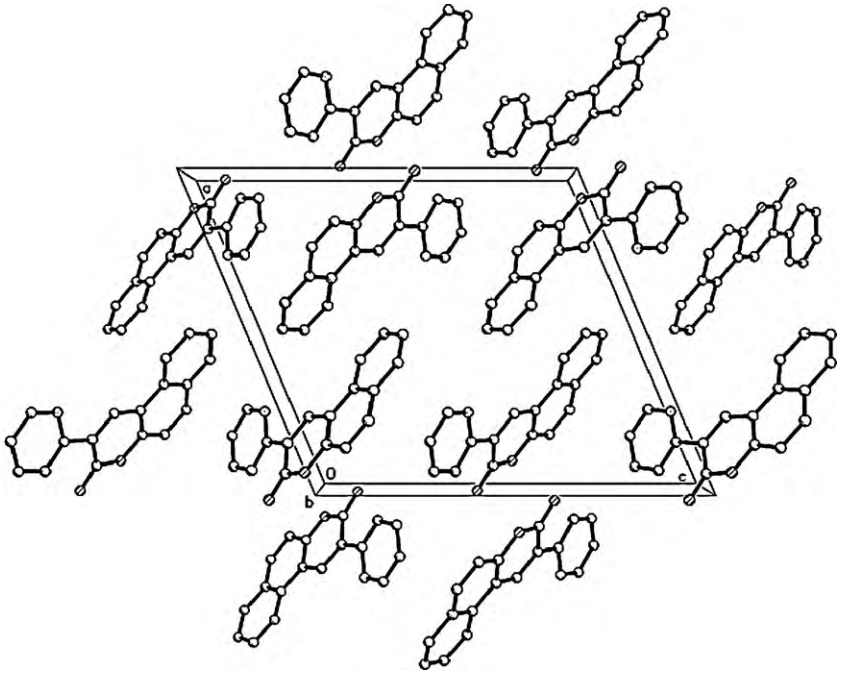

Fig. 4. Packing diagram of PBC. H atoms are omitted for clarity.

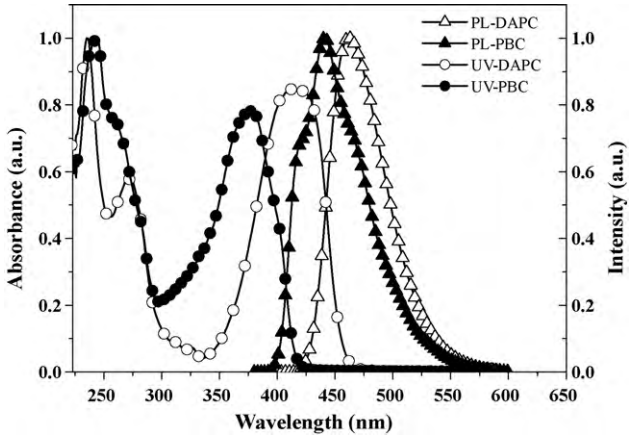

Fig. 5. Normalized UV–vis absorption and emission spectra of DAPC and PBC in diluted dichloromethane solutions ($C = 1 \times 10^{-5}$ mol/L, $\lambda_{ex,DAPC} = 414$ nm, $\lambda_{ex,PBC} = 377$ nm).

higher than these concentrations, the emission intensities were intensively quenched by concentrations of the compounds. The results show that the self-quenchings were occurred.

3.3. Fluorescence quantum yield of the compounds ($\Phi_{F,DAPC}$ and $\Phi_{F,PBC}$)

Fluorescence quantum yields of DAPC ($\Phi_{F,DAPC}$) and PBC ($\Phi_{F,PBC}$) in acetonitrile solutions were measured to be 0.83 and 0.41, respectively. Fluorescence quantum yield of coumarin-6 ($\Phi_{F,Coumarin\,6}$) in acetonitrile is 0.63 [7]. Compared to the commercial coumarin-6 dye, the fluorescence quantum yield of DAPC is higher than that of coumarin-6. From the molecular structures of DAPC and PBC, it was shown that the compound DAPC has an electron-donating diethylamine in the 7-position which enhances the electron density of coumarin ring and enhances the fluorescence quantum yield of the compound, however, the compound PBC has a benzocoumarin skeleton which disperses the electron density of coumarin ring. So the fluorescence quantum yield of DAPC is higher than that of PBC. As shown in crystal structure of coumarin 6 [24], the coumarin moiety is close to planar, the benzothiazolyl moiety is also close to planar. The dihedral angle between the pyrone ring and the thiazolyl ring is 2.30°. From the packing diagram, there is a anti-parallel stacking arrangement of the molecules along *c*-axis, the interplanar distance is approximately 3.3 Å, which means strong intermolecular π–π stacking interaction between coumarin 6 molecules. From the structures of coumarin 6 and DAPC, they all have an electron-attracting moiety (benzothiazolyl and 2-pyridyl) in the 3-position of the coumarin, but the electron attracting ability of 2-pyridyl moiety is different from that of benzothiazolyl moiety. It is likely to the reason for such higher fluorescence quantum yield of DAPC in comparison to coumarin 6.

3.4. Quantum chemical calculations

From the crystal structure of DAPC (Fig. 1), it was found that there were two molecules in the crystal structure. For the sake of quantum chemical calculation, we chose one molecule to optimize DAPC geometrical structure. B3LYP/6-31G(d) optimized structure of DAPC is close to its X-ray crystal structure, B3LYP/6-31G(d) optimized geometrical data of DAPC is in good agreement with the X-ray crystallographic data as listed in Table 2, the average discrepancy of the selected bond lengths between theoretical and experimental data is less than ±0.02 Å, and the average discrepancy of the selected bond angles is less than ±1.5°. Similarly, we also optimize PBC geometrical structure from B3LYP/6-31G(d) calculations, the selected bond lengths and the selected bond angles were listed in Table 2. The results show that the average discrepancies of the selected bond lengths and bond angles between theoretical and experimental data are very small. From Table 2, there are certain discrepancies of the dihedral angles between theoretical and experimental data for DAPC and PBC molecules because we chose the isolated molecules to optimize DAPC and PBC structures and the intermolecular interactions were not involved. However, the actual crystal structures are affected by the solvent and intermolecular interaction.

The HOMO and LUMO levels of DAPC and PBC were deduced using the DFT method as shown in Fig. 7 and Fig. 8, respectively. It can be found that the levels of HOMO and LUMO of DAPC were −5.2237 and −1.6497 eV, and the energy gap between HOMO and LUMO is about 3.574 eV. For PBC, the data were −5.7985, −2.1757 and 3.6228 eV, respectively.

The UV–vis absorption spectra of DAPC and PBC were also calculated by the time-dependent density functional theory (TD-DFT) at the same level. The experimental and calculated data for the lower-lying singlet states of DAPC and PBC were listed in Table 3. As shown in Table 3, there are some discrepancies between theoretical and experimental data due to several influencing factors, such as solvent effect and intermolecular interaction, etc. It has been found that the lowest energy absorptions at 414 nm for DAPC and 377 nm for PBC were due to the electronic $\pi \rightarrow \pi^*$ transition from the HOMO and to the LUMO. For DAPC, the transition occurring at 273 nm was attributed to the electronic $\pi \rightarrow \pi^*$ transition from the HOMO to the LUMO+1 and LUMO+2, the transition occurring at 236 nm was attributed to the electronic $\pi \rightarrow \pi^*$ transition from the HOMO to the LUMO+2. For PBC, the transitions occurring at 264 and 242 nm were attributed to the electronic $\pi \rightarrow \pi^*$ tran-

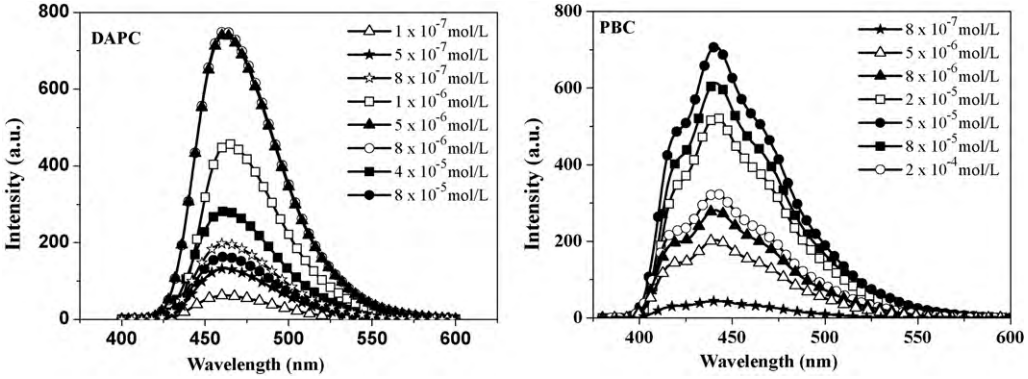

Fig. 6. The emission spectra of DAPC and PBC in diluted dichloromethane solutions at room temperature.

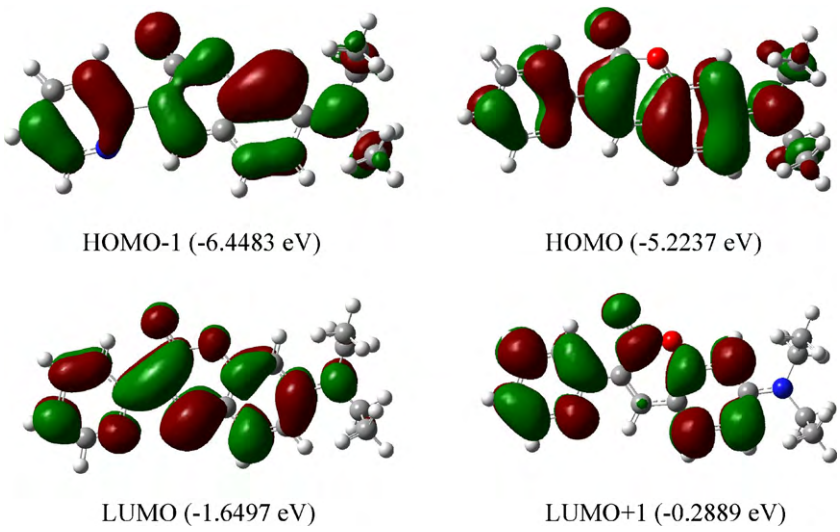

Fig. 7. Frontier molecular orbitals of compound DAPC.

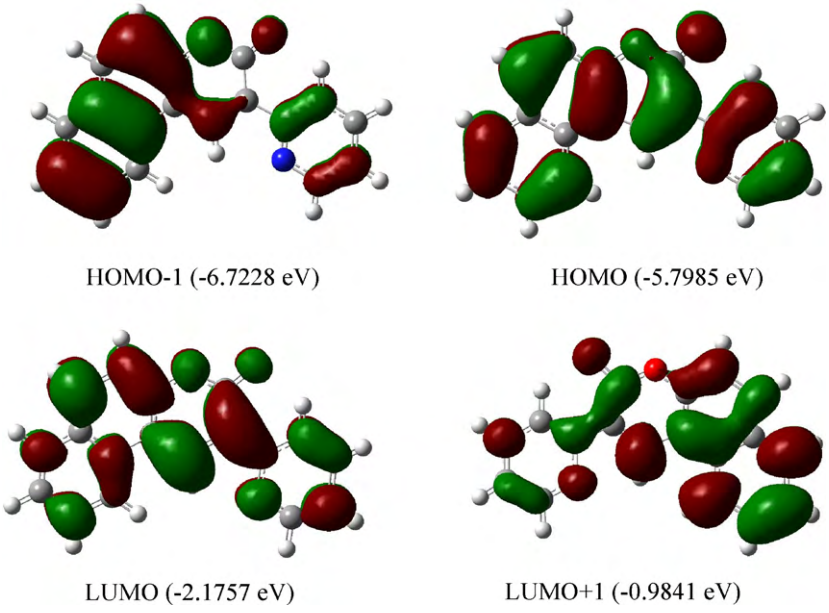

Fig. 8. Frontier molecular orbitals of compound PBC.

Table 3
Absorption spectra data of DAPC and PBC.

Compound	Transition character	OSC[a]	$\lambda_{max,cal.}$ (nm)	$\lambda_{max,exp.}$ (nm)[b]	Transition feature
DAPC	HOMO → LUMO	0.850	371.26	414	$\pi \rightarrow \pi^*$
	HOMO → LUMO+1	0.067	271.63	273	$\pi \rightarrow \pi^*$
	HOMO → LUMO+2	0.080	252.52	236	$\pi \rightarrow \pi^*$
PBC	HOMO → LUMO	0.495	374.48	377	$\pi \rightarrow \pi^*$
	HOMO-1 → LUMO+1	0.067	283.97	264	$\pi \rightarrow \pi^*$
	HOMO-2 → LUMO+2	0.310	231.01	242	$\pi \rightarrow \pi^*$

[a] Oscillator strength coefficients (*f*).
[b] λ_{max} in dichloromethane solvent.

sition from the HOMO-1 to the LUMO+1 and from the HOMO-2 to the LUMO+2, respectively.

4. Conclusions

The new coumarin derivatives, 7-(diethylamino)-3-(pyridin-2-yl)coumarin (DAPC) and 3-(pyridin-2-yl)-benzo[5,6]coumarin (PBC), were successfully synthesized and their photophysical properties have been investigated. Their structures were studied both experimentally and theoretically. The results showed that the compounds exhibit bright blue emission in diluted dichloromethane solutions and the self-quenchings were occurred. There is the strongest blue emission at about concentration of 8.0×10^{-6} mol/L for DAPC and 5.0×10^{-5} mol/L for PBC, respectively. The electron

repelling group (diethylamino) in the 7-position of the coumarin ring causes the shifts of absorption and emission band to longer wavelength. Compared to the compound PBC with benzocoumarin skeleton, the compound DAPC with diethylamino group in the 7-position of the coumarin ring has higher fluorescence quantum yield. DAPC also has higher fluorescence quantum yield in comparison with commercial coumarin-6 and other synthesized coumarin derivatives reported in our literatures.

Supplementary material

The crystallographic data (excluding structure factors) of DAPC and PBC had been deposited with the Cambridge Crystallographic Center as supplementary publication no. CCDC 756576 and no. CCDC 756577, respectively.

Acknowledgements

This work was supported by the Natural Science Foundation of Gansu Province (096RJZA086) and the National Natural Science Foundation of China (Grant 60776006), and also supported by 'Qing Lan' talent engineering funds (QL-05-23A) by Lanzhou Jiaotong University.

References

[1] R.D.H. Murray, J. Mendez, S.A. Brown, The Natural Coumarins: Occurrence. Chemistry and Biochemistry, John Wiley & Sons, New York, 1982.
[2] National Toxicology Program Technical Report on the Toxicology and Carcinogenesis of Coumarin in F344/N Rats and B6C3F$_1$ Mice (Gavage Studies). US Department of Health and Human Services, NIH Publication No. 92-3153, 1992.
[3] R. O'Kennedy, in: R.D. Thornes (Ed.), Coumarins. Biology, Applications and Mode of Action, Wiley, Chichester, 1997.
[4] K.C. Fylaktakidou, D.J. Hadjipavlou-Litina, K.E. Litinas, D.N. Nicolaides, Natural and synthetic coumarin derivatives with anti-inflammatory/antioxidant activities, Curr. Pharm. Des. 10 (2004) 3813–3833.
[5] M. Walshe, J. Howarth, M.T. Kelly, R.O. Kennedy, M.R. Smyth, The preparation of a molecular imprinted polymer to 7-hydroxycoumarin and its use as a solid-phase extraction material, J. Pharm. Biomed. Anal. 16 (1997) 319–325.
[6] S. Sardari, Y. Mori, K. Horita, R.G. Micetich, S. Nishibe, M. Daneshtalab, Synthesis and antifungal activity of coumarins and angular furanocoumarins, Bioorg. Med. Chem. 7 (1999) 1933–1940.
[7] G. Jones, W.R. Jackson, C. Choi, W.R. Bergmark, Solvent effects on emission yield and lifetime for coumarin laser dyes. Requirements for a rotatory decay mechanism, J. Phys. Chem. 89 (1985) 294–300.
[8] D. Ray, P.K. Bharadwaj, A coumarin-derived fluorescence probe selective for magnesium, Inorg. Chem. 47 (2008) 2252–2254.
[9] S.R. Trenor, A.R. Shultz, B.J. Love, T.E. Long, Coumarins in polymers: from light harvesting to photo-cross-linkable tissue scaffolds, Chem. Rev. 104 (2004) 3059–3077.
[10] T.T. Hung, Y.J. Lu, W.Y. Liao, C.L. Huang, Blue violet laser write-once optical disk with coumarin derivative recording layer, IEEE Trans. Magn. 43 (2007) 867–869.
[11] K. Hara, K. Sayama, Y. Ohga, A. Shinpo, S. Suga, H. Arakawa, A coumarin-derivative dye sensitized nanocrystalline TiO_2 solar cell having a high solar-energy conversion efficiency up to 5.6%, Chem. Commun. (2001) 569–570.
[12] (a) T. Hinohara, M. Honda, K. Amano, S. Cho, K. Matsui, Excited states and fluorescence properties of 7-substituted coumarins, Nippon Kagaku Zasshi 4 (1981) 477–480;
(b) L.H. Xu, Y.Y. Zhang, X.L. Wang, J.Y. Chou, Synthesis of styrylcoumarins from coumarin diazonium salts and studies on their spectra characteristics, Dyes Pigm. 62 (2004) 283–289.
[13] J. Griffiths, V. Millar, G.S. Bahra, The influence of chain length and electron acceptor residues in 3-substituted 7-N,N-diethylaminocoumarin dyes, Dyes Pigm. 28 (1995) 327–339.
[14] K. Azuma, S. Suzuki, S. Uchiyama, T. Kajiro, T. Santa, K. Imai, A study of the relationship between the chemical structures and the fluorescence quantum yields of coumarins, quinoxalinones and benzoxazinones for the development of sensitive fluorescent derivatization reagents, Photochem. Photobiol. Sci. 2 (2003) 443–449.
[15] T.Z. Yu, Y.L. Zhao, D.W. Fan, Synthesis, crystal structure and photoluminescence of 3-(1-benzotriazole)-4-methyl-coumarin, J. Mol. Struct. 791 (2006) 18–22.
[16] T.Z. Yu, Y.L. Zhao, X.S. Ding, D.W. Fan, L. Qian, W.K. Dong, Synthesis, crystal structure and photoluminescent behaviors of 3-(1H-benzotriazol-1-yl)-4-methyl-benzo[7,8]coumarin, J. Photochem. Photobiol. A: Chem. 188 (2007) 245–251.
[17] T.Z. Yu, P. Zhang, Y.L. Zhao, H. Zhang, J. Meng, D.W. Fan, L.L. Chen, Y.Q. Qiu, Synthesis, crystal structure and photo- and electro-luminescence of the coumarin derivatives with benzotriazole moiety, Org. Electron. 11 (2010) 41–49.
[18] T.Z. Yu, P. Zhang, Y.L. Zhao, H. Zhang, J. Meng, D.W. Fan, Synthesis, characterization and high-efficiency blue electroluminescence based on coumarin derivatives of 7-diethylamino-coumarin-3-carboxamide, Org. Electron. 10 (2009) 653–660.
[19] H. Zhang, T.Z. Yu, Y.L. Zhao, D.W. Fan, Y.J. Xia, P. Zhang, Y.Q. Qiu, L.L. Chen, Synthesis, crystal structure and photoluminescence of 3-(4-(anthracen-10-yl)phenyl)-benzo[5,6]coumarin, Spectrochim. Acta Part A 75 (2010) 325–329.
[20] S.M. Borisov, I. Klimant, Ultrabright oxygen optodes based on cyclometalated iridium (III) coumarin complexes, Anal. Chem. 79 (2007) 7501–7509.
[21] X.F. Ren, S.Q. Huo, Light emitting device containing phosphorescent complex, WO 2008/010915 A2 (2008).
[22] M. Kaholek, P. Hrdlovič, Characteristics of the excited states of 3-substituted coumarin derivatives and transfer of electronic energy to N-oxyl radicals, J. Photochem. Photobiol. A: Chem. 127 (1999) 45–55.
[23] K.A. Kozyra, J.R. Heldt, H.A. Diehl, J. Heldt, Electronic energy transfer efficiency of mixed solutions of the donor–acceptor pairs: coumarin derivatives—acridine orange, J. Photochem. Photobiol. A: Chem. 152 (2002) 199–205.
[24] J.P. Jasinski, E.S. Paight, 3-(2-Benzothiazolyl)-7-(diethylamino)coumarin, Acta Cryst. C51 (1995) 531–533.